

The hepatic circadian clock is preserved in a lipid-induced mouse model of non-alcoholic steatohepatitis

著者	Ando Hitoshi, Takamura Toshinari, Matsuzawa-Nagata Naoto, Shima Kosuke R., Nakamura Seiji, Kumazaki Masafumi, Kurita Seiichiro, Misu Hirofumi, Togawa Naoyuki, Fukushima Tatsunobu, Fujimura Akio, Kaneko Shuichi
journal or publication title	Biochemical and Biophysical Research Communications
volume	380
number	3
page range	684-688
year	2009-03-13
URL	http://hdl.handle.net/2297/17062

doi: 10.1016/j.bbrc.2009.01.150

**The Hepatic Circadian Clock is Preserved
in a Lipid-induced Mouse Model of Non-Alcoholic Steatohepatitis**

Hitoshi Ando ^{a,b}, Toshinari Takamura ^{a,*}, Naoto Matsuzawa-Nagata ^a,
Kosuke R. Shima ^a, Seiji Nakamura ^a, Masafumi Kumazaki ^a,
Seiichiro Kurita ^a, Hirofumi Misu ^a, Naoyuki Togawa ^c,
Tatsunobu Fukushima ^c, Akio Fujimura ^b, Shuichi Kaneko ^a

^a *Department of Disease Control and Homeostasis, Kanazawa University Graduate School of Medical Science, Kanazawa, Ishikawa 920-8641, Japan*

^b *Department of Pharmacology, School of Medicine, Jichi Medical University, Shimotsuke, Tochigi 329-0498, Japan*

^c *Yokohama Research Laboratories, Mitsubishi Rayon Co., Ltd, Yokohama, Kanagawa 230-0053, Japan*

*Corresponding author. Fax: +81-76-234-4250

E-mail address: ttakamura@m-kanazawa.jp

Abstract

Recent studies have correlated metabolic diseases, such as metabolic syndrome and non-alcoholic fatty liver disease, with the circadian clock. However, whether such metabolic changes *per se* affect the circadian clock remains controversial. To address this, we investigated the daily mRNA expression profiles of clock genes in the liver of a dietary mouse model of non-alcoholic steatohepatitis (NASH) using a custom-made, high-precision DNA chip. C57BL/6J mice fed an atherogenic diet for five weeks developed hypercholesterolemia, oxidative stress, and NASH. DNA chip analyses revealed that the atherogenic diet had a great influence on the mRNA expression of a wide range of genes linked to mitochondrial energy production, redox regulation, and carbohydrate and lipid metabolism. However, the rhythmic mRNA expression of the clock genes in the liver remained intact. Most of the circadianly expressed genes also showed 24-h rhythmicity. These findings suggest that the biological clock is protected against such a metabolic derangement as NASH.

Keywords: Atherogenic diet, Circadian rhythm, Clock gene, Non-alcoholic steatohepatitis, Oxidative stress

Introduction

Various behavioral and physiological processes, including feeding behavior and energy metabolism, exhibit circadian (i.e., 24-h) rhythmicity, which may play a role in maintaining functional homeostasis. Recent studies have revealed that the circadian clock system consists essentially of a set of clock genes [1; 2]. In mammals, the circadian clock resides in the hypothalamic suprachiasmatic nucleus (SCN), which is recognized as being the master clock, and in almost all peripheral tissues [3]. The SCN appears to coordinate peripheral clocks, because it is not essential for driving peripheral oscillations [3].

Rhythmic transcriptional enhancement by two basic helix–loop–helix transcription factors, CLOCK and brain and muscle Arnt-like protein 1 (BMAL1), provides the basic drive for the intracellular clock [1; 2]. In parallel, the heterodimer activates the transcription of various clock-controlled genes. Given that some clock-controlled genes also serve as transcription factors, the expression of numerous genes may be tied to the functions of the circadian clock [1; 2]. For example, nearly half of the known nuclear receptors, including peroxisome proliferator-activated receptors (α , γ , δ) and thyroid hormone receptors (α , β), exhibit circadian expression in liver and adipose tissues, providing a possible explanation for the cyclical behavior of carbohydrate and lipid metabolism [4].

Recent studies have demonstrated relationships between circadian clock function and the development of metabolic diseases, such as type 2 diabetes, metabolic syndrome, and non-alcoholic fatty liver disease (NAFLD). In mice, homozygous mutations in the *Clock* gene lead to the development of metabolic

syndrome [5]. Moreover, we showed that the rhythmic expression of clock genes is blunted in the liver and visceral adipose tissues in KK-A^y mice, a genetic model of obese diabetes [6]. In humans, a similar effect in type 2 diabetes was found in peripheral leukocytes [7]. Furthermore, genetic variations in the *BMAL1* gene are associated with susceptibility to type 2 diabetes and hypertension [8], and *CLOCK* haplotypes are associated with metabolic syndrome [9] and NAFLD [10]. Thus, impairment of the circadian clock appears to contribute to the development of metabolic diseases.

However, whether metabolic diseases *per se* affect the circadian clock remains controversial. High glucose down-regulates mRNA expression of the clock genes (*Per1* and *Per2*) in cultured fibroblasts [11]. Additionally, the DNA-binding activity of the CLOCK-BMAL1 heterodimer is regulated by the redox state, at least *in vitro* [12]. Kohsaka et al. [13] reported that a high-fat diet affected the rhythmic mRNA expression of *Clock*, *Bmal1*, and *Per2* in the liver and adipose tissues of mice. Considering these findings, alterations in glucose, lipid, and energy metabolism; redox state; and/or the concentrations of humoral factors, such as plasma glucose, appear to influence the peripheral circadian clock. However, Oishi et al. [14] demonstrated that clock function was preserved, to a large degree, in the livers, hearts, and kidneys of mice with streptozotocin-induced insulinopenic diabetes. We also revealed that the circadian clock is hardly impaired in the liver and adipose tissues of non-obese, mild hyperglycemic Goto-Kakizaki rats [15]. Furthermore, we did not observe impairment of the circadian clock in the liver or adipose tissues of mice fed a high-fat diet, even though the mice developed metabolic syndrome, characterized by obesity, hyperlipidemia, and hyperglycemia

[16]. Although the reasons for these discrepancies among the various studies are unknown, one reason might be differences in the severity of the pathological condition.

Non-alcoholic steatohepatitis (NASH) is an aggressive form of NAFLD, and the liver with steatosis and inflammation develops hepatic insulin resistance, lipotoxicity, oxidative stress, and mitochondrial abnormalities, which lead to hepatic fibrosis or cirrhosis [17]. We recently established a mouse model of NASH, induced by feeding an atherogenic diet [18]. In this model, the atherogenic diet induced steatosis, inflammation, cellular ballooning, stellate cell activation, hepatic insulin resistance, lipid peroxidation, and oxidative stress in the liver; it finally caused hepatic cirrhosis. Thus, the pathological conditions in the liver of this model are complex and quite severe compared with those of mice fed a simple high-fat diet [13] [16]. Therefore, it is reasonable to expect that the hepatic circadian clock may be impaired in this model, if the alterations in metabolism and redox state affect the oscillator. To test this, we developed a custom-made, high-precision DNA chip useful for analyzing the metabolic status of the liver and investigated the rhythmic mRNA expression of clock genes and genes linked to carbohydrate and lipid metabolism, energy production, and redox regulation in the livers of mice fed an atherogenic diet.

Materials and Methods

Mice. Male C57BL/6J mice (Charles River Laboratories Japan, Yokohama, Japan) were obtained at five weeks of age and maintained under conditions of controlled temperature and humidity and a 12-h light (08:45–20:45 h)/12-h dark (20:45–08:45 h) cycle. Mice had free access to food and drinking water. After three days of acclimation, the mice were divided into two groups. Half of the mice ($n = 16$) were fed a standard laboratory diet (CRF-1, Oriental Yeast Co., Tokyo, Japan), whereas the others ($n = 16$) were given an atherogenic diet (Research Diets, New Brunswick, NJ) containing 34.3% fat (lard, soybean oil), 25.8% protein (casein, L-cystine), 24.6% carbohydrate (maltodextrin, sucrose), 1.3% cholesterol, 0.5% sodium cholate, 5.7% mineral mixture, 1.5% vitamin mixture, and 6.3% cellulose. After five weeks of feeding, animals were sacrificed to obtain blood and liver samples at the following zeitgeber times (ZT): 0, 6, 12, and 18, in which ZT 0 is defined as lights on and ZT 12 as lights off.

All animal procedures were performed in accordance with the standards set forth in the Guidelines for the Care and Use of Laboratory Animals at the Takara-machi campus of Kanazawa University (Kanazawa, Japan).

Statistical analyses. Differences in the variables and mRNA levels between mice fed the atherogenic diet and control mice were evaluated using Student's t test. The rhythmicity of each gene was assessed using one-way ANOVA. The values are presented as the means \pm SEM, and $P < 0.05$ was deemed to indicate statistical significance. All calculations were performed using SPSS software (version 11 for Windows, SPSS Japan, Tokyo, Japan).

Additional details on methods. For details on the blood chemistry, DNA chip analysis, and real-time quantitative PCR, see Supplemental Materials and Methods.

Results

Development of a custom-made DNA chip suitable for metabolic research.

We established a database of hepatic gene expression profiles in various human diseases, and rodent models of diabetes and/or obesity. The models include patients with type 2 diabetes, with or without obesity [19; 20; 21; 22; 23; 24] and NAFLD [25]; genetic rodent models of type 2 diabetes and/or obesity [6; 26]; diet-induced rodent models of obesity [27]; diet-induced rodent models of NAFLD [18; 28; 29]; and a rodent model of ischemic heart disease (manuscript submitted). We extracted the significantly altered genes in each metabolic pathway both in human diseases and animal models and selected 190 mouse genes linked to the circadian clock, energy production, redox regulation, ROS defense, MAPK cascade, energy and cholesterol metabolism, and protein degradation. Because expression of 70 of these genes was hardly detected in a liver sample (FirstChoice mouse liver total RNA, Applied Biosystems) or was determined differently from the results analyzed by real-time PCR, we used data for the other 120 genes for analyses in this study (Supplemental Table 1). The results of the 120 genes analyzed by the DNA chip strongly correlated with those obtained by real-time PCR (Pearson's correlation coefficient $r = 0.963$, $P < 0.0001$; Supplemental Fig. 2).

Mouse model of NASH induced by feeding an atherogenic diet. As reported previously [18], mice fed an atherogenic diet for five weeks developed NASH, diagnosed based on histology (Supplemental Fig. 3). Serum concentrations of ALT and total cholesterol in mice fed the atherogenic diet were significantly higher than

those in control mice (Table 1). The concentration of d-ROMs was also elevated, suggesting that oxidative stress was induced in the mice on the atherogenic diet.

Global gene expression profile in the livers of mice fed an atherogenic diet.

Consistent with the histological and biochemical findings, the DNA chip analyses revealed that the atherogenic diet had a wide influence on mRNA expression, affecting genes linked to energy production, redox regulation, ROS defense, the MAPK cascade, nuclear receptors, energy and cholesterol metabolism, and protein degradation (Supplemental Table 2). In most of the genes examined, the atherogenic diet decreased transcript levels. Specifically, the mRNA expression for 35 of 47 genes linked to energy production and redox regulation, 11 of 16 energy metabolism-related genes, and five of six cholesterol metabolism-related genes was significantly suppressed at one or more time points. However, there was no significant difference in the hepatic mRNA expression levels of clock genes between the mice fed the atherogenic diet and control mice at any time point (Supplemental Table 2). This finding was verified by real-time quantitative PCR (Fig. 1).

In control mice, the DNA chip analyses detected rhythmic mRNA expression in 31 genes, in addition to the clock genes (Fig. 2, Supplemental Fig. 4 and Supplemental Table 1). As reported previously [16], daily expression profiles of *Cyp7a1* gene were opposite in phase between the groups (Fig. 2D). Additionally, the atherogenic diet dampened the mRNA expression rhythms in two of two genes related to ROS defense and seven of eight genes involved in protein degradation (Fig. 2E, Supplemental Fig. 4A and Supplemental Table 1). However, transcript

levels of most of the genes related to energy production, redox regulation, MAPK cascade, nuclear receptors, and energy and cholesterol metabolism, as well as the clock genes, showed significant 24-h rhythmicity in mice fed the atherogenic diet and in control mice (Fig. 2A-D, Supplemental Fig. 4B and Supplemental Table 1). These results suggest that the circadian clock function is maintained in the livers of mice with NASH, probably due to compensating alterations in the expression of various genes, including ROS defense- and protein degradation-associated genes.

Discussion

Accumulating evidence shows that the circadian clock regulates many physiological functions, such as carbohydrate and lipid metabolism [4], mitochondrial energy production, redox regulation, ROS defense [30; 31], and MAPK activity [32]. Thus, it is not surprising that dysfunction in the circadian clock can cause various disorders, including metabolic syndrome [5] and malignancies [33]. However, whether these pathological conditions *per se* cause impairment of clock function remains to be clarified. In particular, our previous finding [16] that simple fatty liver induced by high-fat feeding had little effect on the hepatic circadian clock in mice differs considerably from the results of Kohsaka et al. [13]. To address this issue, we developed a severe NASH model, with oxidative stress and drastic metabolic changes, and investigated the expression rhythms of the clock genes and metabolism- and inflammation-associated genes in the liver of this animal model.

As expected, the atherogenic diet altered the mRNA expression of various genes related to energy production, redox regulation, the MAPK cascade, and carbohydrate and lipid metabolism. Additionally, these effects on mRNA expression exhibited daily variation; they became marked during the dark/active phase. Because the light condition and daily feeding profile did not differ between mice fed the atherogenic diet and control mice, the daily variation in the intake of the atherogenic diet components may have caused the difference between mRNA expression profiles in the dark and light phases. However, the intracellular clock remained intact under these drastically altered conditions. These results suggest

that the circadian clock is protected against, or not susceptible to, alterations in the intracellular environment, including redox state and metabolism.

Light and dietary intake strongly entrain the master and hepatic clocks, respectively [2; 31]. The master clock in the SCN may synchronize the peripheral oscillators, at least partly via the autonomic nervous system [2]. In this study, the mice with NASH were maintained on a well-regulated 12-h light/12-h dark cycle. Additionally, their daily feeding rhythm did not differ from that of control mice (data not shown). Under this condition, the hepatic clock ticked normally. Kohsaka et al. [13] reported that a high-fat diet lengthened the period of locomotor activity rhythm under constant darkness in mice, but the effect was not detected under a 12-h light/12-h dark cycle. Moreover, night-time restricted feeding can normalize the impaired circadian clock in the livers of db/db mice [34]. These results suggest that the signals induced by light and feeding can entrain the hepatic circadian clock, even in the face of the alterations of metabolism and redox state. The influence of a high-fat diet on the hepatic clock may have been observed by Kohsaka et al. [13], but not us [16], due to differences in daily feeding rhythm, which was dampened in their study but not in ours.

Consistent with the intact intracellular clock, the daily expression rhythms of most circadianly expressed genes examined were preserved in the livers of mice with NASH. However, the 24-h expression rhythms of some genes were blunted or changed by the atherogenic diet. It is interesting that the expression rhythms of genes involved in protein degradation were markedly changed in the mice with NASH. The clock proteins, as well as the other short-lived proteins, are degraded by the ubiquitin-proteasome system [2]. Degradation rates of the clock proteins are

controlled by their phosphorylation [2] and binding to an F-box protein [35]. These post-translational regulation mechanisms may account for the fact that Cry2 protein accumulates with a markedly higher circadian amplitude than *Cry2* mRNA [36]. Further studies are needed to determine whether the degradation rates of clock proteins are altered to compensate for the effects of the atherogenic diet.

In conclusion, the atherogenic diet caused NASH and alterations in the intracellular environment, affecting energy metabolism, protein degradation, and redox state. However, these conditions did not impair the circadian clock or the expression rhythms of most of the genes examined in the liver. These findings provide evidence that the circadian clock is protected against alterations in the intracellular environment, including metabolism and redox state. The impairment of biological clock appears to be important as a cause of metabolic disease.

Acknowledgment

This work was supported by in part of a Grant-in-Aid for Scientific Research from the Ministry of Education, Culture, Sports, Science and Technology, Japan.

References

- [1] P.L. Lowrey, and J.S. Takahashi, Mammalian circadian biology: elucidating genome-wide levels of temporal organization. *Annu Rev Genomics Hum Genet* 5 (2004) 407-41.
- [2] S.M. Reppert, and D.R. Weaver, Coordination of circadian timing in mammals. *Nature* 418 (2002) 935-41.
- [3] S.H. Yoo, S. Yamazaki, P.L. Lowrey, K. Shimomura, C.H. Ko, E.D. Buhr, S.M. Sieppka, H.K. Hong, W.J. Oh, O.J. Yoo, M. Menaker, and J.S. Takahashi, *PERIOD2::LUCIFERASE* real-time reporting of circadian dynamics reveals persistent circadian oscillations in mouse peripheral tissues. *Proc Natl Acad Sci U S A* 101 (2004) 5339-46.
- [4] X. Yang, M. Downes, R.T. Yu, A.L. Bookout, W. He, M. Straume, D.J. Mangelsdorf, and R.M. Evans, Nuclear receptor expression links the circadian clock to metabolism. *Cell* 126 (2006) 801-10.
- [5] F.W. Turek, C. Joshu, A. Kohsaka, E. Lin, G. Ivanova, E. McDearmon, A. Laposky, S. Losee-Olson, A. Easton, D.R. Jensen, R.H. Eckel, J.S. Takahashi, and J. Bass, Obesity and metabolic syndrome in circadian Clock mutant mice. *Science* 308 (2005) 1043-5.
- [6] H. Ando, H. Yanagihara, Y. Hayashi, Y. Obi, S. Tsuruoka, T. Takamura, S. Kaneko, and A. Fujimura, Rhythmic messenger ribonucleic acid expression of clock genes and adipocytokines in mouse visceral adipose tissue. *Endocrinology* 146 (2005) 5631-6.
- [7] H. Ando, T. Takamura, N. Matsuzawa-Nagata, K.R. Shima, T. Eto, H. Misu, M.

- Shiramoto, T. Tsuru, S. Irie, A. Fujimura, and S. Kaneko, Clock gene expression in peripheral leucocytes of patients with type 2 diabetes. *Diabetologia* 52 (2008) 329-35.
- [8] P.Y. Woon, P.J. Kaisaki, J. Braganca, M.T. Bihoreau, J.C. Levy, M. Farrall, and D. Gauguier, Aryl hydrocarbon receptor nuclear translocator-like (BMAL1) is associated with susceptibility to hypertension and type 2 diabetes. *Proc Natl Acad Sci U S A* 104 (2007) 14412-7.
- [9] E.M. Scott, A.M. Carter, and P.J. Grant, Association between polymorphisms in the Clock gene, obesity and the metabolic syndrome in man. *Int J Obes (Lond)* 32 (2008) 658-62.
- [10] S. Sookoian, G. Castano, C. Gemma, T.F. Gianotti, and C.J. Pirola, Common genetic variations in CLOCK transcription factor are associated with nonalcoholic fatty liver disease. *World J Gastroenterol* 13 (2007) 4242-8.
- [11] T. Hirota, T. Okano, K. Kokame, H. Shirotani-Ikejima, T. Miyata, and Y. Fukada, Glucose down-regulates Per1 and Per2 mRNA levels and induces circadian gene expression in cultured Rat-1 fibroblasts. *J Biol Chem* 277 (2002) 44244-51.
- [12] J. Rutter, M. Reick, L.C. Wu, and S.L. McKnight, Regulation of clock and NPAS2 DNA binding by the redox state of NAD cofactors. *Science* 293 (2001) 510-4.
- [13] A. Kohsaka, A.D. Laposky, K.M. Ramsey, C. Estrada, C. Joshi, Y. Kobayashi, F.W. Turek, and J. Bass, High-fat diet disrupts behavioral and molecular circadian rhythms in mice. *Cell Metab* 6 (2007) 414-21.
- [14] K. Oishi, M. Kasamatsu, and N. Ishida, Gene- and tissue-specific alterations of

- circadian clock gene expression in streptozotocin-induced diabetic mice under restricted feeding. *Biochem Biophys Res Commun* 317 (2004) 330-4.
- [15] H. Ando, K. Ushijima, H. Yanagihara, Y. Hayashi, T. Takamura, S. Kaneko, and A. Fujimura, Clock Gene Expression in the Liver and Adipose Tissues of Non-Obese Type 2 Diabetic Goto-Kakizaki Rats. *Clin Exp Hypertens* (in press).
- [16] H. Yanagihara, H. Ando, Y. Hayashi, Y. Obi, and A. Fujimura, High-fat feeding exerts minimal effects on rhythmic mRNA expression of clock genes in mouse peripheral tissues. *Chronobiol Int* 23 (2006) 905-14.
- [17] G.C. Farrell, and C.Z. Larter, Nonalcoholic fatty liver disease: from steatosis to cirrhosis. *Hepatology* 43 (2006) S99-S112.
- [18] N. Matsuzawa, T. Takamura, S. Kurita, H. Misu, T. Ota, H. Ando, M. Yokoyama, M. Honda, Y. Zen, Y. Nakanuma, K. Miyamoto, and S. Kaneko, Lipid-induced oxidative stress causes steatohepatitis in mice fed an atherogenic diet. *Hepatology* 46 (2007) 1392-403.
- [19] T. Takamura, M. Sakurai, T. Ota, H. Ando, M. Honda, and S. Kaneko, Genes for systemic vascular complications are differentially expressed in the livers of type 2 diabetic patients. *Diabetologia* 47 (2004) 638-47.
- [20] Y. Takeshita, T. Takamura, E. Hamaguchi, A. Shimizu, T. Ota, M. Sakurai, and S. Kaneko, Tumor necrosis factor-alpha-induced production of plasminogen activator inhibitor 1 and its regulation by pioglitazone and cerivastatin in a nonmalignant human hepatocyte cell line. *Metabolism* 55 (2006) 1464-72.
- [21] H. Misu, T. Takamura, N. Matsuzawa, A. Shimizu, T. Ota, M. Sakurai, H.

- Ando, K. Arai, T. Yamashita, M. Honda, T. Yamashita, and S. Kaneko, Genes involved in oxidative phosphorylation are coordinately upregulated with fasting hyperglycaemia in livers of patients with type 2 diabetes. *Diabetologia* 50 (2007) 268-77.
- [22] Y. Takeshita, T. Takamura, H. Ando, E. Hamaguchi, A. Takazakura, N. Matsuzawa-Nagata, and S. Kaneko, Cross talk of tumor necrosis factor-alpha and the renin-angiotensin system in tumor necrosis factor-alpha-induced plasminogen activator inhibitor-1 production from hepatocytes. *Eur J Pharmacol* 579 (2008) 426-32.
- [23] T. Takamura, H. Misu, N. Matsuzawa-Nagata, M. Sakurai, T. Ota, A. Shimizu, S. Kurita, Y. Takeshita, H. Ando, M. Honda, and S. Kaneko, Obesity Upregulates Genes Involved in Oxidative Phosphorylation in Livers of Diabetic Patients. *Obesity* (in press).
- [24] T. Takamura, H. Misu, T. Yamashita, and S. Kaneko, SAGE application in the study of diabetes. *Curr Pharm Biotechnol* (in press).
- [25] A. Shimizu, T. Takamura, N. Matsuzawa, S. Nakamura, S. Nabemoto, Y. Takeshita, H. Misu, S. Kurita, M. Sakurai, M. Yokoyama, Y. Zen, M. Sasaki, Y. Nakanuma, and S. Kaneko, Regulation of adiponectin receptor expression in human liver and a hepatocyte cell line. *Metabolism* 56 (2007) 1478-85.
- [26] H. Ando, Y. Oshima, H. Yanagihara, Y. Hayashi, T. Takamura, S. Kaneko, and A. Fujimura, Profile of rhythmic gene expression in the livers of obese diabetic KK-A(y) mice. *Biochem Biophys Res Commun* 346 (2006) 1297-302.

- [27] N. Matsuzawa-Nagata, T. Takamura, H. Ando, S. Nakamura, S. Kurita, H. Misu, T. Ota, M. Yokoyama, M. Honda, K. Miyamoto, and S. Kaneko, Increased oxidative stress precedes the onset of high-fat diet-induced insulin resistance and obesity. *Metabolism* (in press).
- [28] M. Uno, S. Kurita, H. Misu, H. Ando, T. Ota, N. Matsuzawa-Nagata, Y. Kita, S. Nabemoto, H. Akahori, Y. Zen, Y. Nakanuma, S. Kaneko, and T. Takamura, Tranilast, an antifibrogenic agent, ameliorates a dietary rat model of nonalcoholic steatohepatitis. *Hepatology* 48 (2008) 109-18.
- [29] S. Kurita, T. Takamura, T. Ota, N. Matsuzawa-Nagata, Y. Kita, M. Uno, S. Nabemoto, K. Ishikura, H. Misu, H. Ando, Y. Zen, Y. Nakanuma, and S. Kaneko, Olmesartan ameliorates a dietary rat model of non-alcoholic steatohepatitis through its pleiotropic effects. *Eur J Pharmacol* 588 (2008) 316-24.
- [30] R. Hardeland, A. Coto-Montes, and B. Poeggeler, Circadian rhythms, oxidative stress, and antioxidative defense mechanisms. *Chronobiol Int* 20 (2003) 921-62.
- [31] S. Langmesser, and U. Albrecht, Life time-circadian clocks, mitochondria and metabolism. *Chronobiol Int* 23 (2006) 151-7.
- [32] K. Obrietan, S. Impey, and D.R. Storm, Light and circadian rhythmicity regulate MAP kinase activation in the suprachiasmatic nuclei. *Nat Neurosci* 1 (1998) 693-700.
- [33] L. Fu, H. Pelicano, J. Liu, P. Huang, and C. Lee, The circadian gene *Period2* plays an important role in tumor suppression and DNA damage response in vivo. *Cell* 111 (2002) 41-50.

- [34] T. Kudo, M. Akiyama, K. Kuriyama, M. Sudo, T. Moriya, and S. Shibata, Night-time restricted feeding normalises clock genes and Pai-1 gene expression in the db/db mouse liver. *Diabetologia* 47 (2004) 1425-36.
- [35] L. Busino, F. Bassermann, A. Maiolica, C. Lee, P.M. Nolan, S.I. Godinho, G.F. Draetta, and M. Pagano, SCFFbx13 controls the oscillation of the circadian clock by directing the degradation of cryptochrome proteins. *Science* 316 (2007) 900-4.
- [36] D. Gatfield, and U. Schibler, *Physiology*. Proteasomes keep the circadian clock ticking. *Science* 316 (2007) 1135-6.

Table 1. Metabolic Parameters in Mice Fed a Regular or Atherogenic Diet

Parameter	Control	Atherogenic	<i>P</i>
Body weight (g)	28.7 ± 0.8	23.2 ± 0.9	< 0.01
Blood glucose (mg/dL)	166 ± 5	163 ± 8	0.73
Serum ALT (U/L)	18 ± 1	51 ± 7	< 0.01
Serum total cholesterol (mg/dL)	98 ± 2	151 ± 7	< 0.01
Serum HDL-cholesterol (mg/dL)	71 ± 2	71 ± 3	0.90
Serum triglyceride (mg/dL)	80 ± 13	14 ± 2	< 0.01
d-ROMs (U)	20 ± 1	34 ± 3	< 0.01

Blood samples were obtained from non-fasted mice at zeitgeber time 0 and 12 ($n = 4$ for each time point in both groups).

Data are means ± SEM of 8 mice.

ALT, Alanine aminotransferase; HDL, high-density lipoprotein; d-ROMs, derivatives of reactive oxygen metabolites.

Figure Legends

Figure 1.

Daily mRNA expression profiles of clock genes in the livers of mice fed a regular (black circles) or an atherogenic (white circles) diet. Transcript levels of the clock genes were determined by real-time quantitative PCR. Data are means \pm SEM of four mice at each time point and are expressed as relative values to the lowest values in control mice for each gene.

Figure 2.

Daily mRNA expression profiles of the circadianly expressed genes related to the MAPK cascade (A), nuclear receptors (B), energy metabolism (C), cholesterol metabolism (D), and protein degradation (E) in the livers of mice fed a regular (black circles) or an atherogenic (white circles) diet. Transcript levels of the clock genes were determined by the custom-made, high-precision DNA chip. Data are means \pm SEM of four mice at each time point and are expressed as relative values to the lowest value in control mice for each gene. * $P < 0.05$, ** $P < 0.01$, vs. control mice.

Supplemental Table 1. Rhythmicity of Hepatic mRNA Expression in Mice Fed a Regular or Atherogenic Diet

				Control		Atherogenic	
Gene Symbol	Description	Accession Code	<i>F</i>	<i>P</i>	<i>F</i>	<i>P</i>	
Energy Production and Redox Regulation							
Nox4	NADPH oxidase 4	NM_015760.2	19.2	0.000	10.3	0.001	
Atp6v1e1	VATPase, H+ transporting, lysosomal V1 subunit E1	NM_007510.2	10.1	0.001	5.3	0.015	
Cyp2e1	cytochrome P450, family 2, subfamily e, polypeptide 1	NM_021282.2	7.4	0.005	3.5	0.050	
Acox2	acyl-Coenzyme A oxidase 2, branched chain	NM_053115.1	6.4	0.008	4.1	0.032	
Uqcrc2	ubiquinol cytochrome c reductase core protein 2	NM_025899.2	4.4	0.026	11.5	0.001	
Uqcr	ubiquinol-cytochrome c reductase (6.4kD) subunit	NM_025650.2	3.9	0.036	2.1	0.149	
Atp5c1	ATP synthase, H+ transporting, mitochondrial F1 complex, gamma polypeptide 1	NM_020615.2	3.6	0.046	1.9	0.185	
Atp5o	ATP synthase, H+ transporting, mitochondrial F1 complex, O subunit	NM_138597.2	3.4	0.052	4.1	0.032	
Atp6v0b	ATPase, H+ transporting, lysosomal V0 subunit B	NM_033617.1	3.4	0.055	1.4	0.304	
Atp6v1f	ATPase, H+ transporting, lysosomal V1 subunit F	NM_025381.1	3.2	0.060	5.1	0.017	
Atp6v1h	ATPase, H+ transporting, lysosomal V1 subunit H	NM_133826.2	3.1	0.066	2.9	0.077	
Slc25a5	solute carrier family 25 (mitochondrial carrier, adenine nucleotide translocator), member 5	NM_007451.2	2.8	0.086	4.1	0.033	
Ndufs8	NADH dehydrogenase (ubiquinone) Fe-S protein 8	NM_144870.3	2.8	0.088	2.8	0.083	
Ndufv1	NADH dehydrogenase (ubiquinone) flavoprotein 1	NM_133666.2	2.7	0.095	5.4	0.014	
Ndufs1	NADH dehydrogenase (ubiquinone) Fe-S protein 1	NM_145518.1	2.4	0.121	4.9	0.019	
Atp6v0d1	ATPase, H+ transporting, lysosomal V0 subunit D1	NM_013477.2	2.0	0.168	0.2	0.874	
Ndufa6	NADH dehydrogenase (ubiquinone) 1 alpha subcomplex, 6 (B14)	NM_025987.1	1.9	0.185	2.1	0.149	
Ndufa7	NADH dehydrogenase (ubiquinone) 1 alpha subcomplex, 7 (B14.5a)	NM_023202.2	1.8	0.195	3.7	0.042	
Cox4i1	cytochrome c oxidase subunit IV isoform 1	NM_009941.2	1.8	0.196	1.2	0.364	
Cox5b	cytochrome c oxidase, subunit Vb	NM_009942.2	1.8	0.210	1.3	0.310	
Ndufs2	NADH dehydrogenase (ubiquinone) Fe-S protein 2	NM_153064.3	1.7	0.211	2.7	0.096	
Uqcrcs1	ubiquinol-cytochrome c reductase, Rieske iron-sulfur polypeptide 1	NM_025710.1	1.6	0.234	1.7	0.212	
Ndufa2	NADH dehydrogenase (ubiquinone) 1 alpha subcomplex, 2	NM_010885.2	1.6	0.244	2.3	0.124	

Supplemental Table 1. (continued)

	Gene Symbol	Description	Accession Code	Control		Atherogenic	
				<i>F</i>	<i>P</i>	<i>F</i>	<i>P</i>
	Cox17	cytochrome c oxidase, subunit XVII assembly protein homolog (yeast)	NM_001017429.2	1.6	0.251	0.4	0.744
	Ndufb10	NADH dehydrogenase (ubiquinone) 1 beta subcomplex, 10	NM_026684.1	1.5	0.268	0.3	0.857
	Ndufa3	NADH dehydrogenase (ubiquinone) 1 alpha subcomplex, 3	NM_025348.1	1.5	0.271	2.6	0.104
	Ndufv2	NADH dehydrogenase (ubiquinone) flavoprotein 2	NM_028388.1	1.5	0.274	1.6	0.244
	Atp5a1	ATP synthase, H ⁺ transporting, mitochondrial F1 complex, alpha subunit, isoform 1	NM_007505.1	1.4	0.298	1.4	0.281
	Ndufa4	NADH dehydrogenase (ubiquinone) 1 alpha subcomplex, 4	NM_010886.1	1.4	0.300	2.0	0.173
	Sco1	SCO cytochrome oxidase deficient homolog 1 (yeast)	NM_001040026.1	1.4	0.304	17.7	0.000
	Sdha	succinate dehydrogenase complex, subunit A, flavoprotein (Fp)	NM_023281.1	1.3	0.307	1.3	0.313
	Atp5b	ATP synthase, H ⁺ transporting mitochondrial F1 complex, beta subunit	NM_016774.2	1.3	0.328	1.3	0.328
	Cox6a1	cytochrome c oxidase, subunit VI a, polypeptide 1	NM_007748.3	1.2	0.361	12.0	0.001
	Acox3	acyl-Coenzyme A oxidase 3, pristanoyl	NM_030721.2	1.1	0.379	5.8	0.011
	Acox1	acyl-Coenzyme A oxidase 1, palmitoyl	NM_015729.2	1.0	0.430	1.3	0.328
	Sdhc	succinate dehydrogenase complex, subunit C, integral membrane protein	NM_025321.1	1.0	0.436	2.0	0.161
	Cox5a	cytochrome c oxidase, subunit Va	NM_007747.2	0.9	0.470	1.4	0.290
	Uqcrb	ubiquinol-cytochrome c reductase, complex III subunit VII	NM_026219.1	0.9	0.484	0.9	0.449
	Atp5e	ATP synthase, H ⁺ transporting, mitochondrial F1 complex, epsilon subunit	NM_025983.3	0.8	0.502	1.3	0.308
	Cyp4a12	cytochrome P450, family 4, subfamily a, polypeptide 12	NM_177406.3	0.8	0.515	0.8	0.539
	Atp6ap1	ATPase, H ⁺ transporting, lysosomal accessory protein 1	NM_018794.2	0.8	0.532	1.0	0.424
	Atp6v1b2	ATPase, H ⁺ transporting, lysosomal V1 subunit B2	NM_007509.2	0.8	0.538	6.6	0.007
	Cyp4a10	cytochrome P450, family 4, subfamily a, polypeptide 10	NM_010011.2	0.7	0.580	0.8	0.522
	Ndufb4	NADH dehydrogenase (ubiquinone) 1 beta subcomplex 4	NM_026610.1	0.7	0.595	1.2	0.337
	Cox7c	cytochrome c oxidase, subunit VIIc	NM_007749.3	0.5	0.714	0.9	0.471
	Uqcrc1	ubiquinol-cytochrome c reductase core protein 1	NM_025407.2	0.5	0.717	1.6	0.249
	Atp5j	ATP synthase, H ⁺ transporting, mitochondrial F0 complex, subunit F	NM_016755.2	0.2	0.908	0.7	0.550

Supplemental Table 1. (continued)							
				Control		Atherogenic	
Gene Symbol	Description	Accession Code	<i>F</i>	<i>P</i>	<i>F</i>	<i>P</i>	
ROS Defense							
Gss	glutathione synthetase	NM_008180.1	5.7	0.012	3.4	0.054	
Gsr	glutathione reductase 1	NM_010344.3	4.3	0.028	1.8	0.194	
Sod1	superoxide dismutase 1, soluble	NM_011434.1	2.4	0.122	3.5	0.050	
Cat	catalase	NM_009804.1	2.1	0.157	2.3	0.129	
Txn1	thioredoxin 1	NM_011660.2	1.8	0.194	0.5	0.668	
Prdx1	peroxiredoxin 1	NM_011034.2	1.6	0.252	2.0	0.172	
Sod3	superoxide dismutase 3, extracellular	NM_011435.3	1.5	0.272	3.0	0.073	
Gpx3	glutathione peroxidase 3	NM_008161.1	1.5	0.275	4.5	0.024	
Sod2	superoxide dismutase 2, mitochondrial	NM_013671.3	1.3	0.305	2.6	0.099	
Gsta4	glutathione S-transferase 4	NM_010357.1	1.3	0.305	6.9	0.006	
Gpx1	glutathione peroxidase 1	NM_008160.2	0.8	0.542	1.6	0.240	
MAPK Cascade							
Map2k3	mitogen-activated protein kinase kinase 3	NM_008928.1	12.6	0.001	10.9	0.001	
Nfkbia	nuclear factor of kappa light polypeptide gene enhancer in B-cells inhibitor, alpha	NM_010907.1	10.5	0.001	9.2	0.002	
Mknk2	MAP kinase interacting serine/threonine kinase 2	NM_021462.2	7.1	0.005	3.3	0.058	
Araf	v-raf murine sarcoma 3611 viral oncogene homolog	NM_009703.1	3.7	0.043	20.9	0.000	
Hras1	v-Ha-ras Harvey rat sarcoma viral oncogene homolog	NM_008284.1	3.1	0.068	0.7	0.567	
Mapkapk2	MAP kinase-activated protein kinase 2	NM_008551.1	2.5	0.112	0.3	0.826	
Cebpa	CCAAT/enhancer binding protein (C/EBP), alpha	NM_007678.2	1.3	0.311	2.3	0.129	
Map2k5	mitogen-activated protein kinase kinase 5	NM_011840.2	1.2	0.369	9.1	0.002	
Jun	v-jun sarcoma virus 17 oncogene homolog (avian)	NM_010591.1	0.9	0.479	3.9	0.037	
Map3k3	mitogen-activated protein kinase kinase kinase 3	NM_011947.1	0.6	0.616	3.4	0.052	
Grb2	growth factor receptor-bound protein 2	NM_008163.3	0.1	0.981	1.4	0.293	

Supplemental Table 1. (continued)							
				Control		Atherogenic	
Gene Symbol	Description	Accession Code	<i>F</i>	<i>P</i>	<i>F</i>	<i>P</i>	
Clock Genes							
Arntl	brain and muscle Arnt-like protein 1 (BMAL1)	NM_007489.3	90.7	0.000	61.0	0.000	
Clock	clock	NM_007715.5	37.1	0.000	18.0	0.000	
Cry1	cryptochrome 1	NM_007771.3	23.2	0.000	38.3	0.000	
Per1	period 1	NM_011065.2	11.4	0.001	10.7	0.001	
Per2	period 2	NM_011066.1	8.2	0.003	40.1	0.000	
Cry2	cryptochrome 2	NM_009963.3	5.3	0.015	4.4	0.027	
Nuclear Receptors							
Ppard	peroxisome proliferator activator receptor delta	NM_011145.3	25.8	0.000	49.3	0.000	
Ppara	peroxisome proliferator activated receptor alpha	NM_011144.2	8.3	0.003	5.6	0.012	
Nr1i2	nuclear receptor subfamily 1, group I, member 2 (PXR)	NM_010936.1	3.6	0.047	5.5	0.013	
Srebf1	sterol regulatory element binding factor 1	NM_011480.1	2.9	0.082	3.8	0.039	
Nr1h4	nuclear receptor subfamily 1, group H, member 4 (FXR)	NM_009108.1	2.1	0.150	2.5	0.111	
Nr0b2	nuclear receptor subfamily 0, group B, member 2 (SHP)	NM_011850.2	2.1	0.159	2.5	0.107	
Pparg	peroxisome proliferator activated receptor gamma	NM_011146.1	1.7	0.224	3.3	0.056	
Nr1h3	nuclear receptor subfamily 1, group H, member 3 (LXRa)	NM_013839.2	1.2	0.356	2.6	0.100	
Energy Metabolism							
Cpt1a	carnitine palmitoyltransferase 1a, liver	NM_013495.1	14.0	0.000	4.7	0.022	
Gck	glucokinase	NM_010292.4	11.0	0.001	5.5	0.013	
Pck1	phosphoenolpyruvate carboxykinase 1	NM_011044.2	7.4	0.005	5.7	0.012	
Dgat2	diacylglycerol O-acyltransferase 2	NM_026384.3	4.9	0.019	6.5	0.007	
G6pc	glucose 6-phosphatase	NM_008061.3	3.1	0.068	2.1	0.160	
Pklr	pyruvate kinase	NM_013631.1	3.0	0.073	1.9	0.182	
Scd1	stearoyl-Coenzyme A desaturase 1	NM_009127.3	2.6	0.102	2.4	0.117	

Supplemental Table 1. (continued)							
	Gene Symbol	Description	Accession Code	Control		Atherogenic	
				<i>F</i>	<i>P</i>	<i>F</i>	<i>P</i>
	Fasn	fatty acid synthase	NM_007988.3	2.3	0.127	4.0	0.035
	Dgat1	diacylglycerol O-acyltransferase 1	NM_010046.2	2.0	0.162	4.3	0.027
	Pfkl	phosphofructokinase	NM_008826.2	1.6	0.247	3.0	0.072
	Gpd1	glycerol-3-phosphate dehydrogenase	NM_010271.2	1.4	0.303	5.1	0.017
	Cpt2	carnitine palmitoyltransferase 2	NM_009949.1	1.3	0.317	1.1	0.387
	Acads	acyl-Coenzyme A dehydrogenase, short chain	NM_007383.2	1.2	0.338	7.3	0.005
	Acaca	Acetyl-Coenzyme A carboxylase alpha	NM_133360.1	0.9	0.484	1.1	0.392
	Hadha	Hydroxyacyl-CoA dehydrogenase, alpha subunit	NM_178878.1	0.9	0.492	1.3	0.314
	Acadm	acyl-Coenzyme A dehydrogenase, medium chain	NM_007382.1	0.8	0.501	2.8	0.083
Cholesterol Metabolism							
	Abcc2	ATP-binding cassette, sub-family C, member 2 (MRP2)	NM_013806.2	11.3	0.001	8.4	0.003
	Hmgcs1	3-hydroxy-3-methylglutaryl-Coenzyme A synthase 1	NM_145942.2	9.2	0.002	6.0	0.010
	Cyp7a1	cytochrome P450, family 7, subfamily a, polypeptide 1	NM_007824.2	4.9	0.019	4.1	0.031
	Hmgcr	3-hydroxy-3-methylglutaryl-Coenzyme A reductase	NM_008255.1	3.3	0.057	5.3	0.015
	Cyp27a1	cytochrome P450, family 27, subfamily a, polypeptide 1	NM_024264.3	2.2	0.142	2.5	0.107
	Ldlr	low density lipoprotein receptor	NM_010700.2	1.1	0.380	0.7	0.579
Protein Degradation							
	Psma5	proteasome subunit, alpha type 5	NM_011967.2	11.4	0.001	0.9	0.477
	Psma1	proteasome subunit, alpha type 1	NM_011965.1	11.0	0.001	1.0	0.431
	Ubc	ubiquitin	NM_019639.3	7.2	0.005	2.7	0.095
	Psmb2	proteasome subunit, beta type 2	NM_011970.2	6.8	0.006	9.5	0.002
	Psmd1	proteasome 26S subunit, non-ATPase, 1	NM_027357.1	4.2	0.030	1.0	0.428
	Psma3	proteasome subunit, alpha type 3	NM_011184.2	3.9	0.038	3.1	0.065
	Psmb1	proteasome subunit, beta type 1	NM_011185.2	3.8	0.039	0.2	0.925

Supplemental Table 1. (continued)							
Gene Symbol	Description	Accession Code	Control		Atherogenic		
			<i>F</i>	<i>P</i>	<i>F</i>	<i>P</i>	
Psme1	proteasome 28 subunit, alpha	NM_011189.1	3.8	0.040	0.4	0.781	
Tnfsf5ip1	Proteasome assembling protein 2 (PAC2)	NM_134138.1	3.0	0.073	4.2	0.030	
Psme2	proteasome 28 subunit, beta	NM_011190.3	1.9	0.184	0.7	0.565	
Psmd2	proteasome 26S subunit, non-ATPase, 2	NM_134101.1	1.9	0.187	3.2	0.062	
Psmb5	proteasome subunit, beta type 5	NM_011186.1	1.7	0.217	3.8	0.039	
Psmd14	proteasome 26S subunit, non-ATPase, 14	NM_021526.1	1.0	0.406	2.0	0.165	
Dscr2	proteasome assembling protein 1 (PAC1)	NM_019537.1	0.3	0.806	2.1	0.148	
Psme3	proteaseome 28 subunit, 3	NM_011192.3	0.1	0.950	0.3	0.795	

Liver samples were obtained from mice at ZT 0, 6, 12, and 18 ($n = 4$ for each time point in both groups).

The rhythmicity of each gene was tested using one-way ANOVA.

Supplemental Table 2. Effects of the Atherogenic Diet on Hepatic mRNA Expression											
	Gene	ZT0	ZT6	ZT12	ZT18		Gene	ZT0	ZT6	ZT12	ZT18
Energy Production and Redox Regulation											
	Cyp4a12	0.22**	0.28**	0.17**	0.30**		Ndufa2	0.87**	0.88	0.82*	0.79*
	Acox1	0.57**	0.54**	0.47**	0.56*		Atp6v0d1	0.89*	0.88	0.82**	0.92
	Sdha	0.72**	0.74**	0.71*	0.75*		Ndufa4	0.86*	0.89	0.85	0.80*
	Ndufb10	0.72**	0.78**	0.74*	0.73*		Slc25a5	0.79**	0.92	0.95	0.84
	Uqcrc1	0.73**	0.75**	0.79*	0.70*		Uqcrb	0.83**	0.86	0.84	0.80
	Ndufs1	0.74**	0.81**	0.79*	0.69*		Atp5c1	0.83**	0.93	0.86	0.85
	Uqcr	0.74**	0.79**	0.71**	0.68**		Ndufb4	0.85*	0.87	0.96	0.85
	Ndufv1	0.75**	0.79**	0.65**	0.65**		Ndufa7	0.87	0.92	0.80*	0.80**
	Ndufs2	0.75**	0.79**	0.77*	0.71**		Sco1	0.92	0.96	0.81**	0.68**
	Sdhc	0.77**	0.78**	0.78*	0.71**		Atp5j	0.91	0.86	0.91	0.82*
	Atp5b	0.77**	0.83*	0.79*	0.75*		Acox3	0.98	0.89	0.92	0.72*
	Atp5a1	0.77**	0.82*	0.79*	0.78*		Cyp4a10	0.63	0.44	0.38	0.45
	Ndufa6	0.79**	0.87*	0.79*	0.73*		Atp6v1h	0.88	1.07	1.09	0.98
	Cox6a1	0.79**	0.81**	0.62**	0.63**		Cox5a	0.89	0.94	0.97	0.93
	Cox5b	0.80**	0.81**	0.72**	0.77*		Cox17	0.95	0.95	0.98	1.03
	Uqcrc2	0.80**	0.76**	0.72**	0.71**		Cyp2e1	0.98	0.99	0.99	1.04
	Cox4i1	0.81**	0.87*	0.79*	0.78*		Acox2	1.00	0.94	1.08	0.91
	Cox7c	0.82*	0.85**	0.83*	0.78*		Atp6v0b	1.01	1.06	0.87	0.89
	Uqcrfs1	0.79**	0.83*	0.84*	0.80		Atp6v1e1	1.13	1.21†	1.08	1.17†
	Atp5o	0.80**	0.84**	0.82	0.75*		Atp6v1f	1.16††	1.11	1.04	1.07
	Atp5e	0.86*	0.85*	0.91	0.80*		Atp6ap1	1.18††	1.15	1.19	1.18
	Ndufs8	0.86*	0.90*	0.89	0.78*		Nox4	1.48††	1.29††	1.14	1.19
	Ndufv2	0.75**	0.85*	0.85	0.85		Atp6v1b2	1.51†	1.44††	1.29††	1.26
	Ndufa3	0.86**	0.90	0.85*	0.78*						
ROS Defense											
	Sod1	0.72**	0.73**	0.63**	0.64**		Gpx3	1.14	0.99	1.12	0.99
	Cat	0.73**	0.70**	0.64*	0.70*		Gsta4	1.19	1.14	1.18	1.14
	Sod2	0.73**	0.76**	0.81*	0.81		Gss	1.22	1.03	0.81	0.99
	Prdx1	1.00	0.93	0.83*	0.88		Txn1	1.34††	1.13	1.19	1.32
	Gsr	1.04	0.90	0.88	0.97		Sod3	1.93††	1.49	1.47	1.48
	Gpx1	1.12	1.05	0.96	1.05						
MAPK Cascade											
	Cebpa	0.67*	0.74**	0.65**	0.59**		Map2k5	1.20	1.27	1.08	1.00
	Araf	0.77**	0.82*	0.69*	0.60**		Map3k3	1.33	1.32†	1.42†	1.14
	Hras1	0.97	1.03	0.82	0.71*		Nfkbia	1.48†	1.23	1.50†	1.41
	Map2k3	1.01	1.17	0.90	0.70**		Grb2	1.46††	1.49†	1.33††	1.27
	Mknk2	1.03	1.10	0.78	0.63*		Mapkapk2	1.22†	1.32††	1.49††	1.53†
	Jun	1.00	1.01	1.42	0.83						

Supplemental Table 2. (continued)											
	Gene	ZT0	ZT6	ZT12	ZT18		Gene	ZT0	ZT6	ZT12	ZT18
Clock Genes											
	Clock	1.08	1.01	1.10	0.94		Cry2	1.10	1.17	1.05	0.96
	Arntl	1.05	0.84	0.93	1.03		Per1	1.22	1.57	1.11	0.95
	Cry1	1.04	0.92	1.15	0.99		Per2	0.83	1.10	1.02	0.92
Nuclear Receptors											
	Pparg	0.57	0.55	0.35**	0.26*		Nr1h3	1.01	1.03	1.02	0.91
	Nr1h4	0.66**	0.84	0.80**	0.65*		Ppara	1.21	1.01	0.84	0.84
	Nr1i2	0.86	0.78*	0.90	0.79		Srebf1	1.47	1.99††	1.34	1.25
	Ppard	0.85	1.13	1.10	0.95		Nr0b2	1.66†	1.23	1.02	1.72
Energy Metabolism											
	Fasn	0.27*	0.40*	0.42*	0.38**		Cpt2	0.79**	0.82	0.82	0.81
	Gpd1	0.44**	0.50**	0.36**	0.40**		Pfk1	0.94	0.99	0.93	0.78*
	Gck	0.46**	1.16	0.68	0.51**		Acaca	0.73	0.85	0.75	0.56**
	Hadha	0.74**	0.75*	0.65**	0.65*		Acadm	0.82	0.84	0.89	0.79
	Acads	0.75**	0.80*	0.68**	0.63*		Dgat1	0.93	0.89	0.82	0.78
	Dgat2	0.76**	0.87*	0.79	0.60**		G6pc	1.10	0.73	0.85	1.62
	Pklr	0.51**	0.65*	0.68	0.52**		Cpt1a	1.17	0.90	0.83	0.97
	Scd1	0.67*	1.27	0.88	0.84		Pck1	1.68	0.88	0.97	1.40
Cholesterol Metabolism											
	Hmgcs1	0.22**	0.26**	0.36**	0.29*		Cyp7a1	0.39**	1.55	0.80	0.42*
	Ldlr	0.47**	0.51**	0.54**	0.43**		Cyp27a1	0.75**	0.73**	0.78*	0.71*
	Hmgcr	0.49**	0.52**	0.54*	0.29**		Abcc2	0.98	1.08	1.17	1.26
Protein Degradation											
	Psme3	0.74*	0.63**	0.65**	0.65**		Psmb2	1.03	1.01	0.91	0.96
	Psmd1	0.93	0.74*	0.83	0.84		Psmd14	1.08	0.93	0.88	1.08
	Psmb5	0.92	0.97	0.87	0.84*		Psma1	1.14	0.98	1.06	1.26††
	Dscr2	0.93	0.93	0.91	0.83*		Psma5	1.18†	0.99	1.02	1.37†
	Ubc	0.87	1.01	1.02	1.05		Psme1	1.49††	1.32	1.37††	1.41
	Tnfsf5ip1	0.96	1.03	1.04	0.98		Psma3	1.12†	1.16†	1.01	1.11†
	Psmd2	0.98	0.90	0.85	0.89		Psme2	1.48††	1.36††	1.49†	1.64†
	Psmb1	1.02	0.91	0.87	0.99						
Data are shown as ratio of mean mRNA expression level in mice fed the atherogenic diet to that in control mice.											
$n = 4$ for each time point in both groups.											
Compared with control mice, significantly decreased: * $P < 0.05$, ** $P < 0.01$; significantly increased: † $P < 0.05$, †† $P < 0.01$.											
ZT, zeitgeber time.											

Figure 1

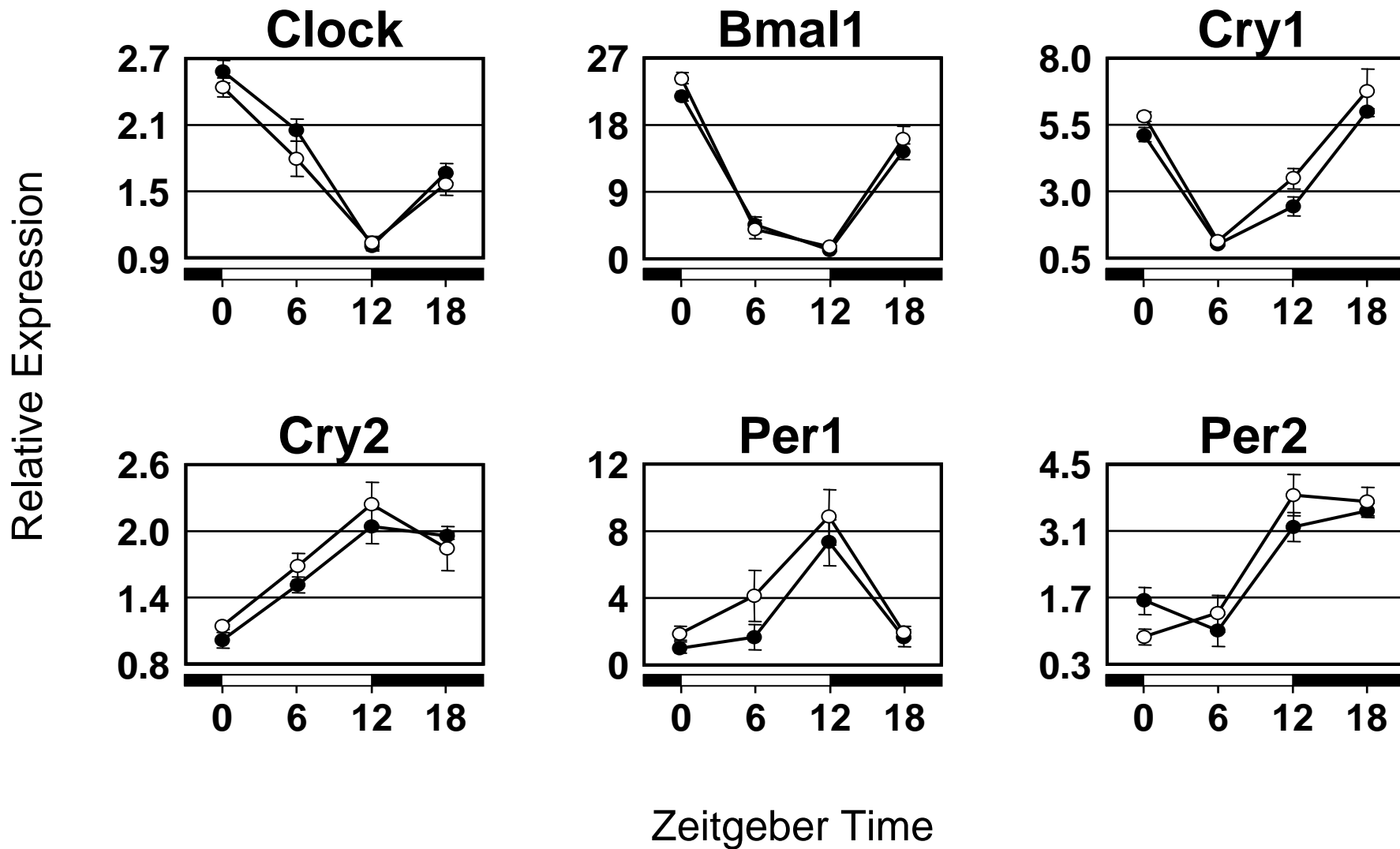
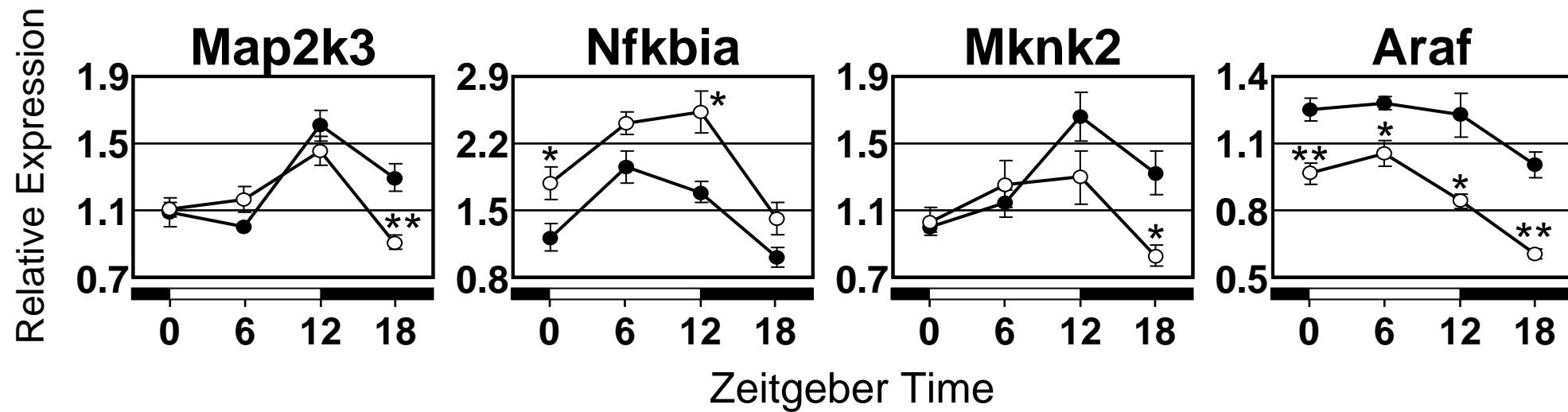


Figure 2

A



B

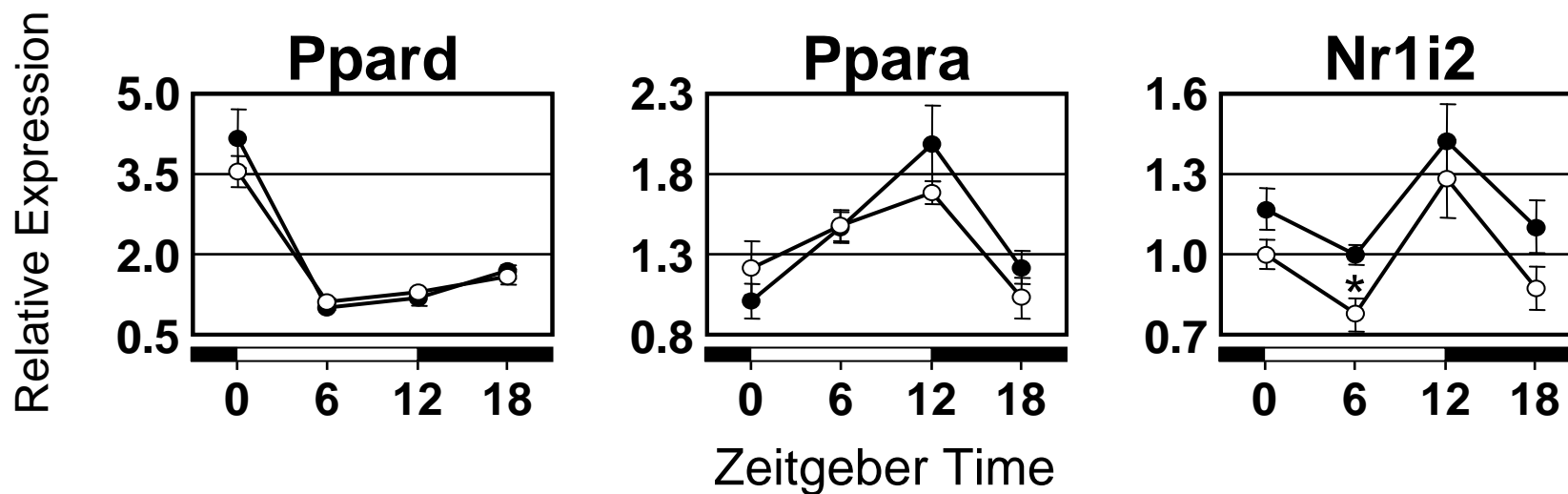
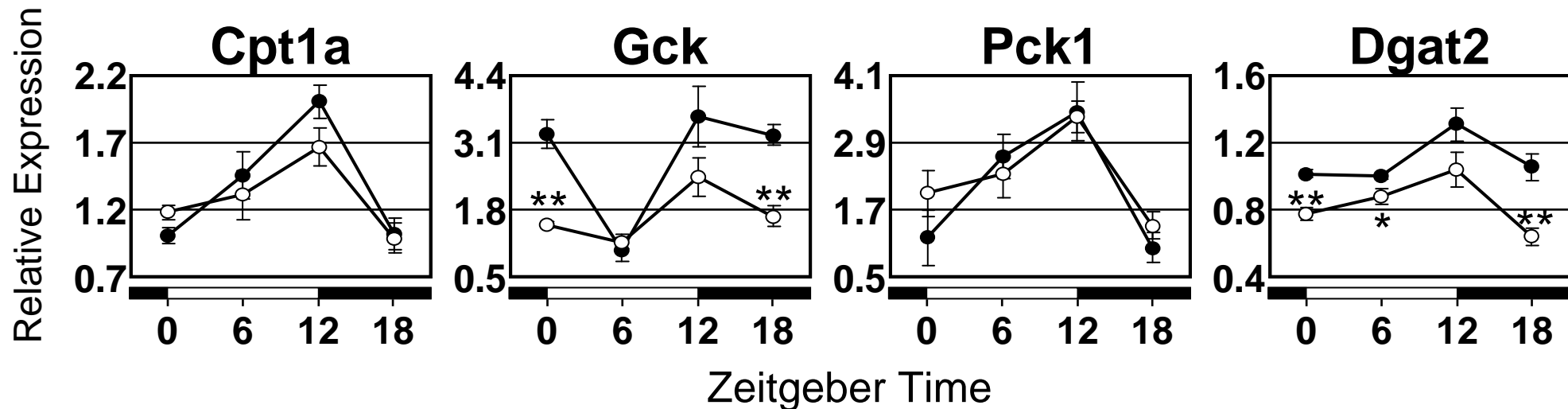


Figure 2

C



D

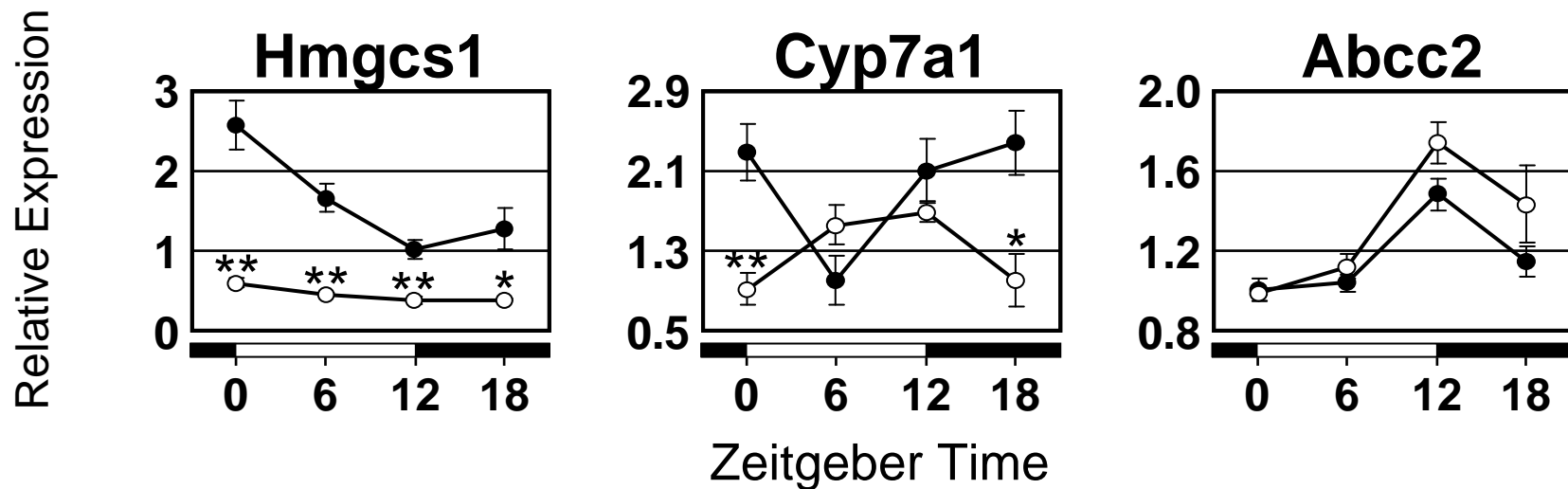
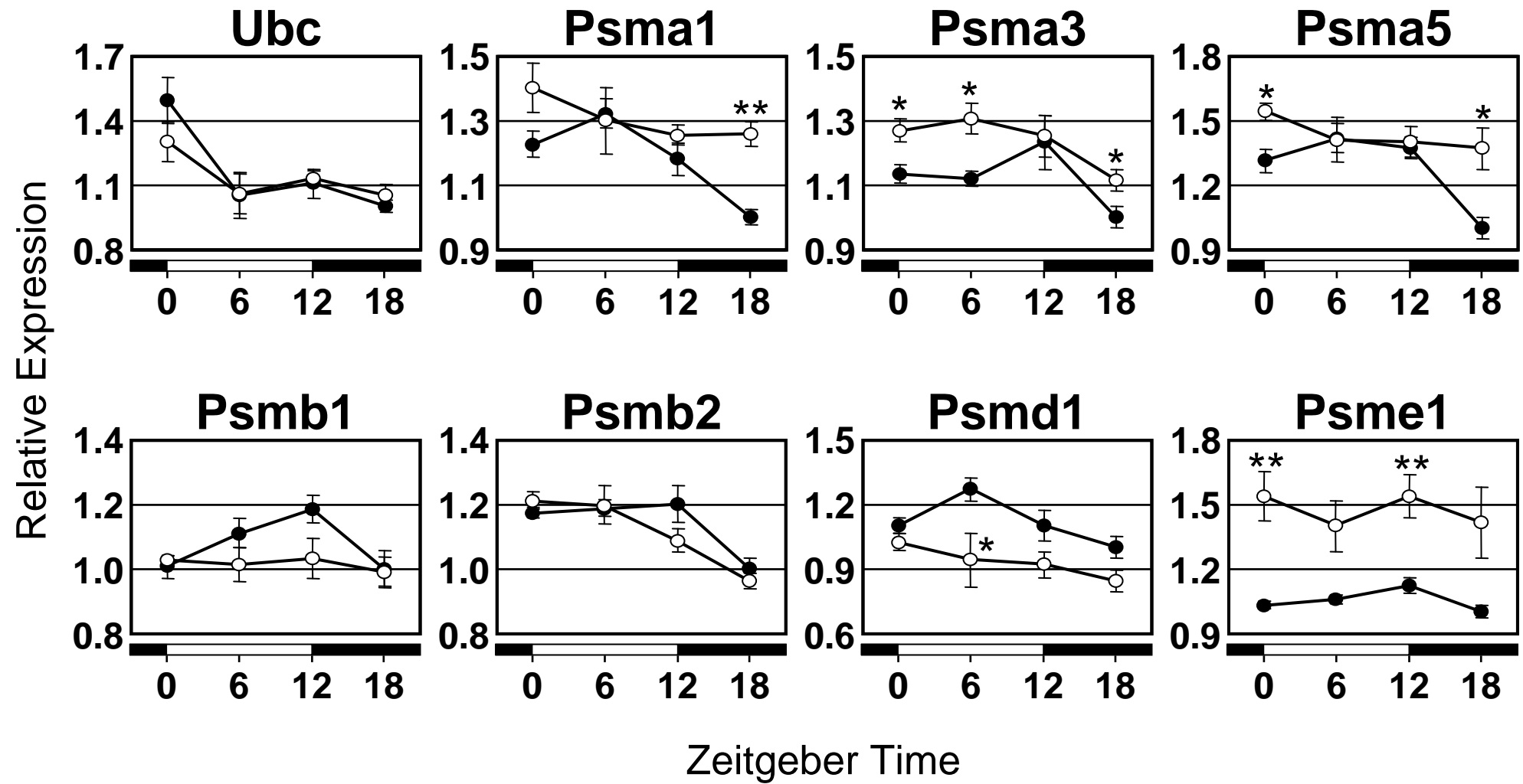


Figure 2

E



Supplemental Materials and Methods

Blood chemistry. Blood glucose concentration was measured using the FreeStyle system (Kissei Pharmaceutical Co., Matsumoto, Japan). Assays for serum alanine aminotransferase (ALT) and total cholesterol were performed using reagents purchased from Kanto Chemical Co. (Tokyo, Japan) and Sysmex (Kobe, Japan), respectively. Serum triglyceride and high-density lipoprotein (HDL)-cholesterol concentrations were assayed using commercial kits (Sekisui Medical Co., Tokyo, Japan). The serum concentration of derivatives of reactive oxygen metabolites (d-ROMs), a marker of oxidative stress, was measured using a previously described method [37]. The intra- and interassay coefficients of variation were all < 10%.

DNA chips. We designed 65mer oligonucleotide DNA probes for 190 mouse genes linked to circadian clock, energy production, redox regulation, reactive oxygen species (ROS) defense, mitogen-activated protein kinase (MAPK) cascade, energy and cholesterol metabolism, and protein degradation using ProbeQuest software (Dynacom Co., Mobarra, Japan). The sequence of the probe for each gene was selected considering melting temperature, specificity, secondary structure, and low complexity sequences and was located within 1000 bases from the 3'-end of mRNA sequences. Melting temperatures of designed probes were between 70°C and 80°C. Synthesized probes were installed onto Genopal (Mitsubishi Rayon Co., Tokyo, Japan; Supplemental Fig. 1; <http://www.mrc.co.jp/genome/e/index.html>), which consists of hollow plastic fibers. In this system, oligonucleotide DNA probes are immobilized to a hydrophilic gel within the three-dimensional space of each

hollow fiber [38, 39].

RNA isolation and DNA chip analysis. Total RNA was extracted from liver samples using the RNeasy Mini Kit (Qiagen, Valencia, CA). All total RNA samples were analyzed using an Agilent 2100 bioanalyzer (Agilent Technologies, Palo Alto, CA) for quality. Biotinylated antisense RNA was synthesized and amplified from total RNA (1 μ g) using the MessageAmpII biotin enhanced amplification kit (Applied Biosystems, Foster City, CA) according to the manufacturer's protocol. After purification of the aRNA, the biotinylated aRNA (5 μ g) was fragmented using 10 \times fragmentation reagents (Applied Biosystems), by heating at 70°C for 7.5 min.

Hybridization was carried out with the DNA chips in 150 μ L hybridization buffer (0.12 M Tris HCl / 0.12M NaCl / 0.05% Tween-20 and 5 μ g fragmented biotinylated aRNA) at 65°C overnight. After hybridization, the DNA chips were washed twice in 0.12 M Tris HCl / 0.12 M NaCl / 0.05% Tween-20 at 65°C for 20 min, followed by washing in 0.12 M Tris HCl / 0.12M NaCl for 10 min. Then hybridized aRNA was labeled with 2 μ g/mL streptavidin-Cy5 (GE Healthcare, Little Chalfont, UK) in 0.12 M Tris HCl / 0.12 M NaCl for 30 min at room temperature. After fluorescent labeling, the DNA chips were washed four times in 0.12 M Tris HCl / 0.12 M NaCl / 0.05% Tween-20 at room temperature for 5 min each. DNA chips were scanned at multiple exposure times, ranging from 0.1 to 40 s, using a DNA chip reader (Yokogawa Electric, Tokyo, Japan) with multi-beam excitation technology. The intensity values with the best exposure condition for each spot were selected. The median value of background spots was subtracted from the intensity value in each gene, and thereafter the value was normalized to

the expression of an endogenous control, *Arbp* (NM_007475.4).

Real-time quantitative PCR. cDNA was synthesized from total RNA (1 µg) using the High Capacity cDNA Reverse Transcription Kit (Applied Biosystems). Gene expression was analyzed by real-time quantitative PCR using the Applied Biosystems 7500 Fast Real-Time PCR system. All specific sets of primers and TaqMan probes (TaqMan Gene Expression Assays) were obtained from Applied Biosystems. Gene expression levels of the target sequences were normalized to the expression of *Arbp*. Data were analyzed using the comparative threshold cycle method.

References

- [37] G. Buonocore, S. Perrone, M. Longini, L. Terzuoli, and R. Bracci, Total hydroperoxide and advanced oxidation protein products in preterm hypoxic babies. *Pediatr Res* 47 (2000) 221-4.
- [38] M. Kobori, H. Nakayama, K. Fukushima, M. Ohnishi-Kameyama, H. Ono, T. Fukushima, Y. Akimoto, S. Masumoto, C. Yukizaki, Y. Hoshi, T. Deguchi, and M. Yoshida, Bitter gourd suppresses lipopolysaccharide-induced inflammatory responses. *J Agric Food Chem* 56 (2008) 4004-11.
- [39] K. Nagao, N. Togawa, K. Fujii, H. Uchikawa, Y. Kohno, M. Yamada, and T. Miyashita, Detecting tissue-specific alternative splicing and disease-associated aberrant splicing of the PTCH gene with exon junction microarrays. *Hum Mol Genet* 14 (2005) 3379-88.

Supplemental Figure Legends

Supplemental Figure 1.

Features of the fibrous DNA Chip Genopal. Genopal (Mitsubishi Rayon Co., Tokyo, Japan) is a commercially produced, fibrous DNA chip manufactured with the company's unique hollow fiber block slicing method.

Supplemental Figure 2.

Correlation between relative expression levels as determined by the DNA chip and by real-time PCR. The relative expression value of a liver total RNA sample to a mixture of 10-tissue total RNA samples (FirstChoice mouse total RNA, Applied Biosystems) was determined for each gene using both methods. Data are expressed as log₂-transformed values. The correlation was assessed by Pearson's regression analysis.

Supplemental Figure 3.

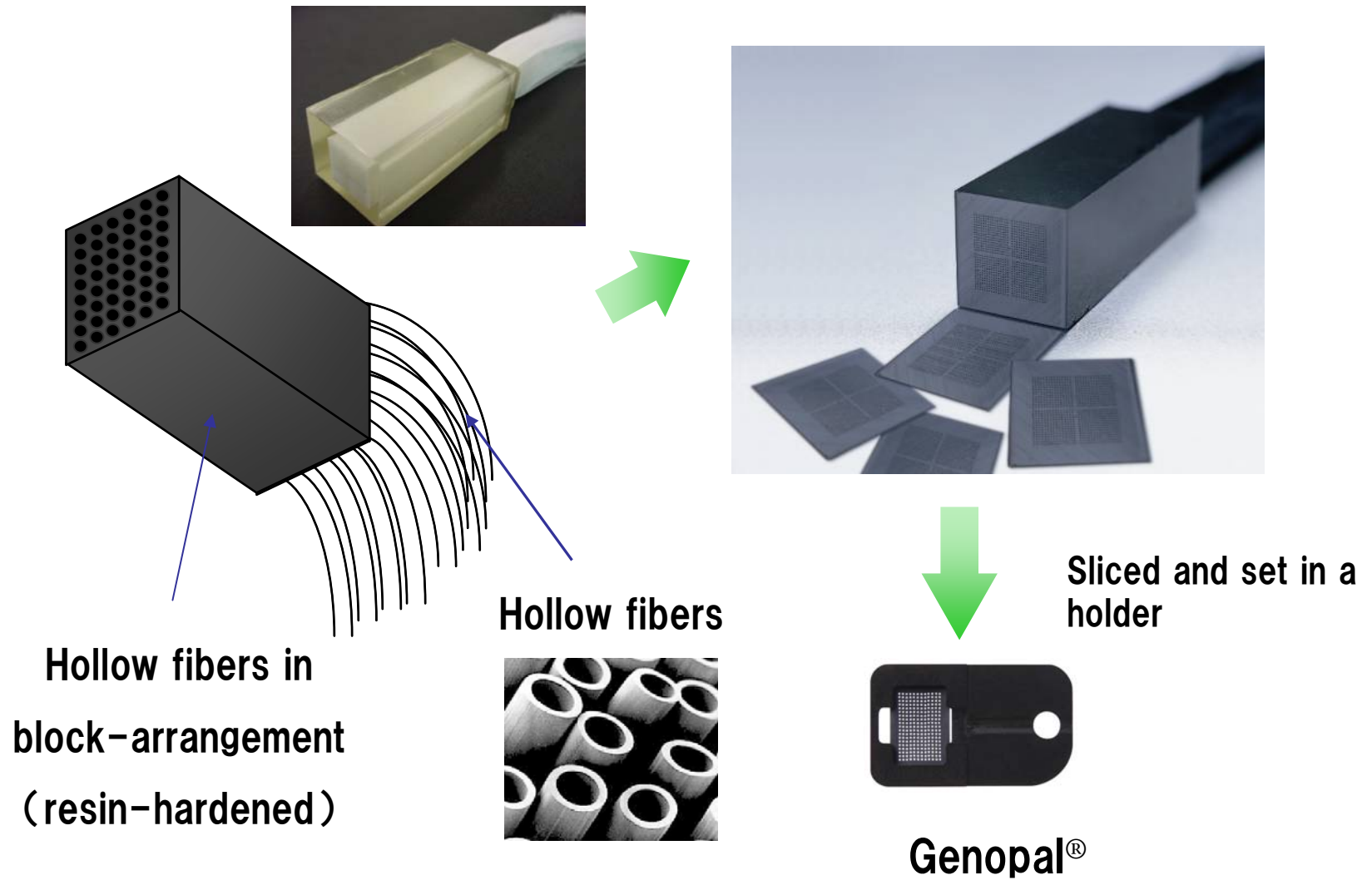
Representative liver histology in 10-week-old mice fed a regular or an atherogenic diet. The atherogenic diet was given from 5 to 10 weeks of age. Liver sections were stained with hematoxylin and eosin. The arrows indicate infiltration of inflammatory cells into the hepatic parenchyma. The scale bars represent 25 μ m.

Supplemental Figure 4.

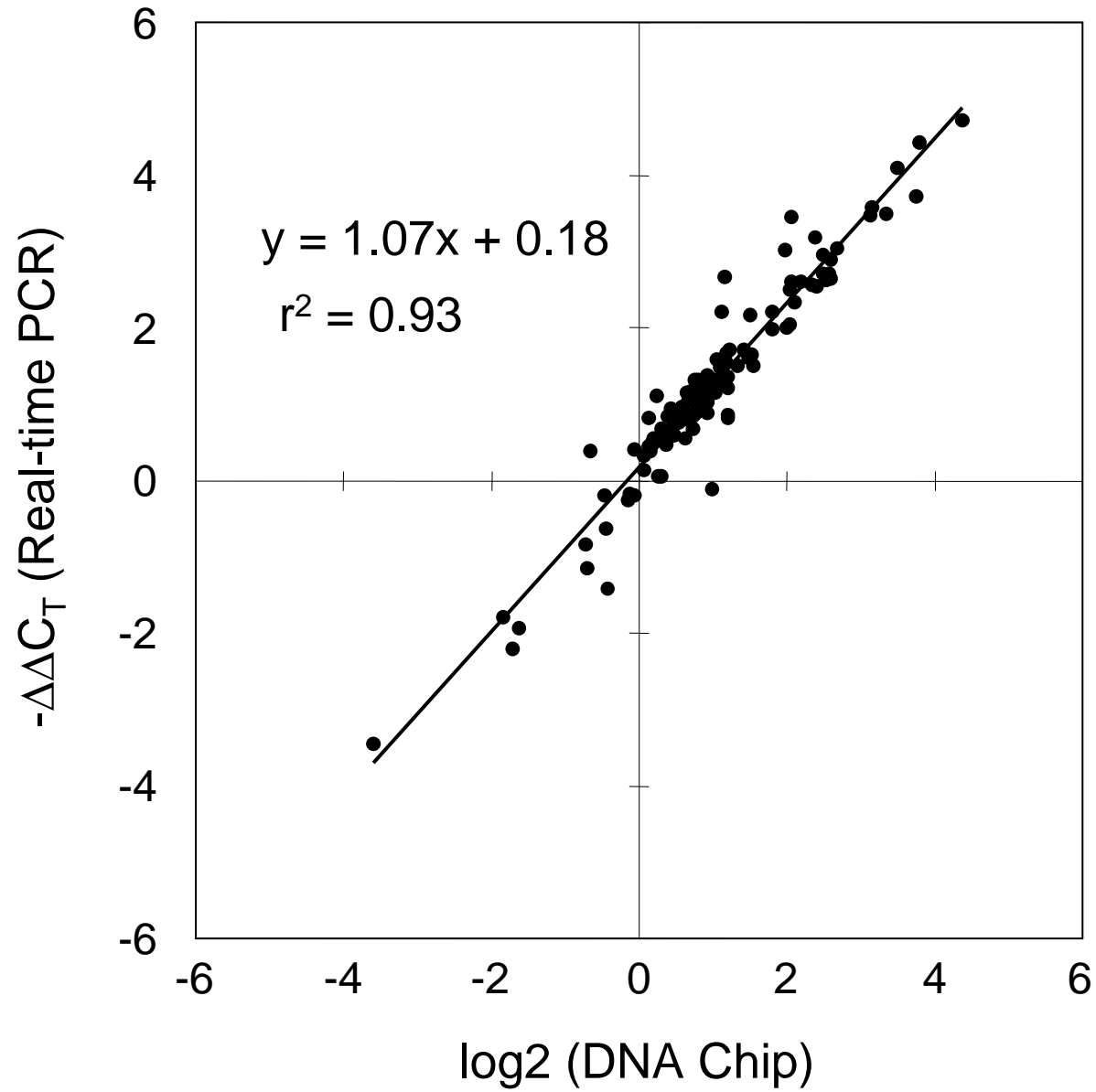
Daily mRNA expression profiles of the circadianly expressed genes related to ROS

defense (A) and energy production and redox regulation (B) in the livers of mice fed a regular (black circles) or an atherogenic (white circles) diet. Transcript levels of the clock genes were determined by the custom-made, high-precision DNA chip. Data are means \pm SEM of four mice at each time point and are expressed as relative values to the lowest value in control mice for each gene. * $P < 0.05$, ** $P < 0.01$, vs. control mice.

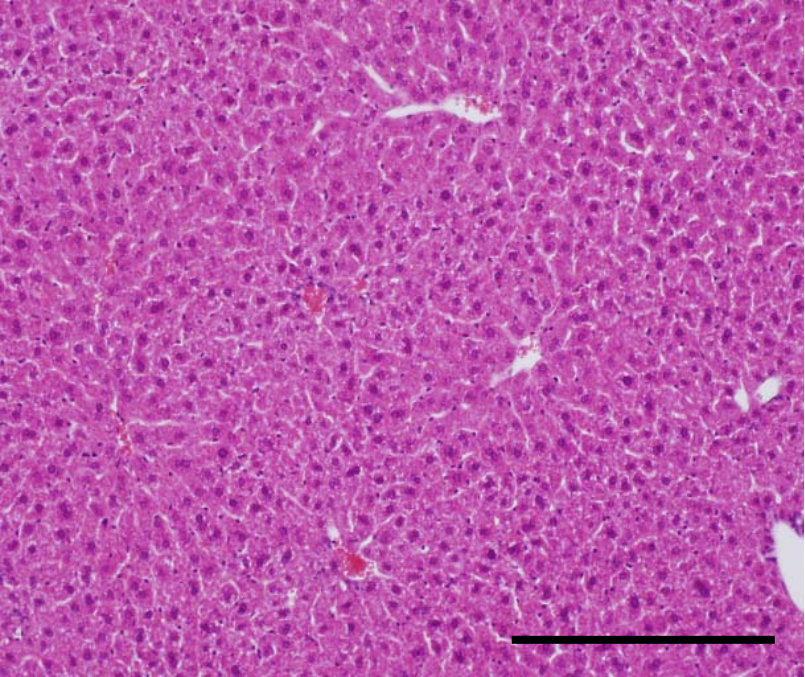
Supplemental Figure 1



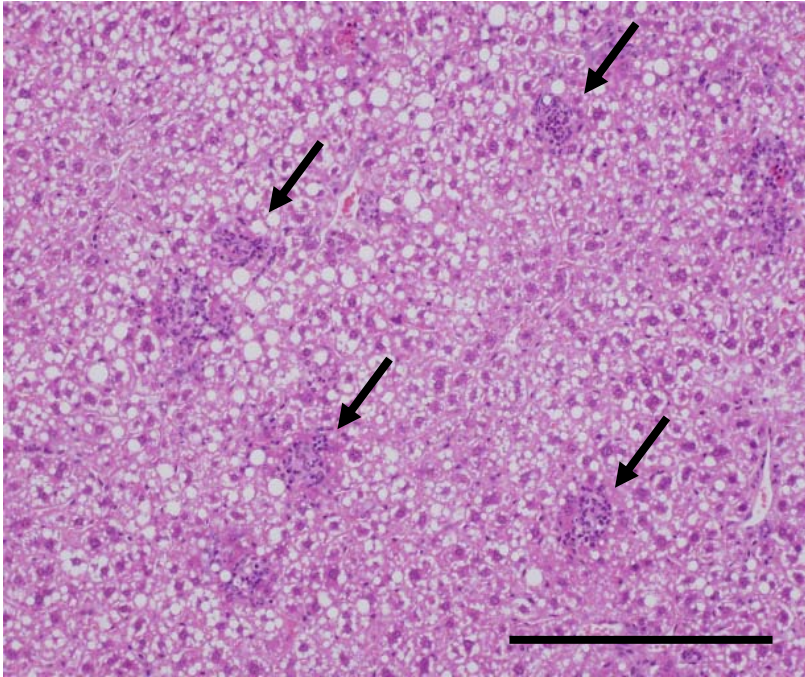
Supplemental Figure 2



Control



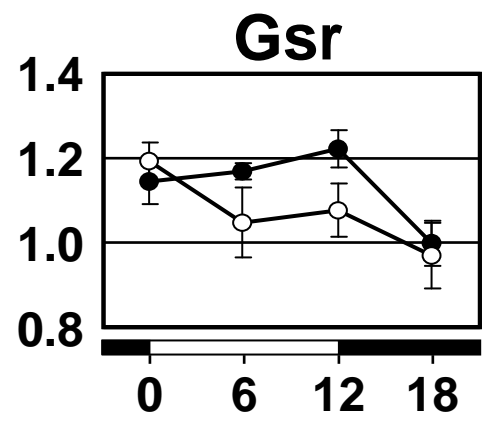
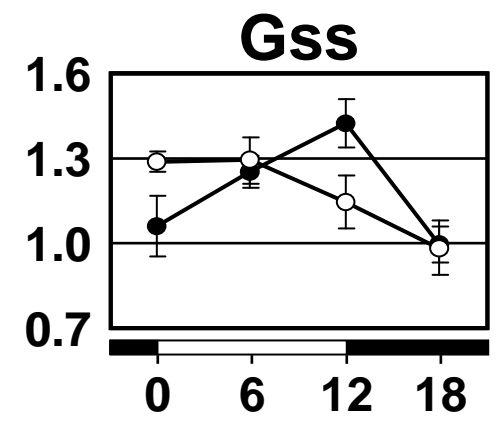
Atherogenic



25microm

A

Relative Expression



Zeitgeber Time

B